The European turbulence code benchmarking effort: turbulence driven by thermal gradients in magnetically confined plasmas

G L Falchetto[1], B D Scott[2], P Angelino[1], A Bottino[2], T Dannert[3], V Grandgirard[1], S Janhunen[4], F Jenko[2], S Jolliet[3], A Kendl[5], B F McMillan[3], V Naulin[6], A H Nielsen[6], M Ottaviani[1], A G Peeters[7], M J Pueschel[2], D Reiser[8], T T Ribeiro[2,10] and M Romanelli[9]

[1] CEA, IRFM, F-13108 Saint-Paul-Lez-Durance, France
[2] Max-Planck-Institut für Plasmaphysik, IPP-Euratom Association, D-85748 Garching, Germany
[3] Centre de Recherches en Physique des Plasmas, Association Euratom - Confédération Suisse, EPFL, CH-1015 Lausanne, Switzerland
[4] Helsinki University of Technology, Euratom - Tekes Association, FIN-02015 TKK, Finland
[5] Institute for Ion Physics and Applied Physics, University of Innsbruck, Association Euratom-ÖAW, A- 6020 Innsbruck, Austria
[6] Risø National Laboratory, DTU, DK-4000 Roskilde, Denmark
[7] University of Warwick, CV4 7AL Coventry, UK
[8] Forschungszentrum Jülich GmbH, Institute of Energy Research, IEF-4:Plasma Physics, Association EURATOM-FZJ 52425 Jülich, Germany
[9] Euratom-UKAEA Fusion Association, Culham Science Centre, Abingdon, UK
[10] Instituto de Plasmas e Fusão Nuclear, Euratom/IST Association, Lisbon, Portugal

E-mail: gloria.falchetto@cea.fr

Abstract

A cross-comparison and verification of state-of-the-art European codes describing gradient-driven plasma turbulence in the core and edge regions of tokamaks, carried out within the EFDA Task Force on Integrated Tokamak Modelling, is presented. In the case of core ion temperature gradient (ITG) driven turbulence with adiabatic electrons (neglecting trapped particles), good/reasonable agreement is found between various gyrokinetic/gyrofluid codes. The main physical reasons for some deviations observed in nonlocal simulations are discussed. The edge simulations agree very well on collisionality scaling and acceptably well on beta scaling (below the MHD boundary) for cold-ion cases, also in terms of the non-linear mode structure.

(Some figures in this article are in colour only in the electronic version)

1. Introduction

The computation of turbulence and transport in magnetized plasmas continues to make rapid advances. Local 'flux-tube' numerical simulations have been available for several years and physically comprehensive versions (all values of collisionality, beta, gyroradii) are feasible now. Global electromagnetic gyrofluid simulations at very large scale ($L \sim 1000$ Larmor radii) are now possible, whereas global electromagnetic gyrokinetic models begin to be affordable. However, since the last major effort 10 years ago [1] there has been only sporadic work to benchmark the various approaches generally and individual implementations ('codes') in particular. The only serious wide scale effort [2, 3] involved electron scale 'hyperfine' turbulence [4]. The establishment of such an effort involving both global and local models within the EFDA Task Force on Integrated Tokamak Modelling (ITM) [5] is reported here. The verification and benchmark of codes (cf glossary in [6]) is a prerequisite to their validation under experimental parameter conditions allowing for the definition of numerical standards which provide a higher degree of confidence in the prediction of transport under ITER conditions.

　　Core turbulence is most often temperature gradient dominated, thus standard test cases have been chosen of pure ion temperature gradient driven (ITG) turbulence with the electrons in parallel force balance ('adiabatic electrons'). Testing of electromagnetic cases is still emerging. For edge turbulence all three main gradients (electron density, electron and ion temperatures) participate in the turbulence drive, but given the persistence of simplified edge models, a standard 'four-field' model reflecting generic electron pressure gradient drive with electromagnetic parallel dynamics is used.

　　The main points describing the advance of the present cross-verification study are as follows. Some of the models themselves are new; these include 'full-f' versions of both particle and Eulerian ('Vlasov') gyrokinetic models, as detailed in section 3. All of the global models evolve the profiles and therefore necessarily follow the self-consistent equilibrium $E \times B$ flow and other neoclassical processes. Some of the models use global field-aligned geometry, which is in no way restricted to short wavelengths or toroidally ballooned mode structure, as in some of the previously benchmarked codes. The use of edge cases and models in a comparison is itself new. For the global codes, the present cross-verification is rigorously carried out on a common prescribed model case (including specified analytical profiles as well as parameters) to avoid discrepancies based on differences in profile shape which affected the preliminary versions (especially for adiabatic core cases, as the density profile is static). In addition to time-trace information of turbulent, or 'anomalous', heat and particle fluxes, the present code comparisons include several elements of the turbulence mode structure, namely spectra of both the fluctuations and the turbulent fluxes and the radial and poloidal envelopes of fluctuations. Any comparison beyond time traces of integrated quantities allows one to distinguish between a level of agreement in a set of numbers and then another level of agreement in the qualitative information which is necessary to the discussion about physical processes. Of course it remains to say that this is a beginning, not an end. In particular, comparisons between electromagnetic gyrokinetic models lie in the future. The present effort opens the way to further investigations which will allow one to move forward in improving the predictive capability of turbulent transport models.

　　The following sections describe the test problems, the set of codes used and the results.

2. Test problems

The originality of this study is the definition, within the framework of the Integrated Tokamak Modelling Task Force Project on Transport and Turbulent processes (IMP♯4) of common

prescribed model problems for the benchmark of global turbulence codes, both for the core and for the edge of a tokamak plasma, as detailed in the following. Numerical simulations are constrained by the test case specifications, which strongly restrict the freedom of authors in the way they treat the model problem itself.

2.1. Core turbulence

The standard test problem chosen for the cross-verification of core turbulence codes is the standard case of hot-ion collisionless ITG driven turbulence, taken from the 'Cyclone Base Case' [1]. The set of parameters, extracted from DIII-D shot 81499, at the reference radius $r_0 = r/a = 0.5$ (*a* being the minor radius) is the following: $n_e = 4.5 \times 10^{19}\,\text{m}^{-3}$, $T_e = T_i = 2 \times 10^3\,\text{eV}$, $B = 1.91\,\text{T}$, $a = 0.625\,\text{m}$, $R = 1.71\,\text{m}$, $L_T = 0.246\,\text{m}^{-1}$, $L_T/L_n = 0.321$, $q = 1.4$, $\hat{s} = 0.78$. R is the major radius, L_n and L_T are density and temperature scale lengths, respectively, q the safety factor and $\hat{s}$ the magnetic shear. The nominal values of normalized ion Larmor radius and temperature scale length for this test case are, respectively, $\rho* \equiv \rho_i/a = 1/184.7$ and $R/L_T = 6.91$.

The benchmark simulations have been performed by local codes using the above parameters, whereas global code simulations have been constrained to use prescribed geometry and initial simulation profiles, designed to provide the nominal values at the given reference radius. A concentric circular cross-section tokamak geometry is chosen (neglecting the Shafranov shift). Given $r_a = r/a$, the radial simulation domain is $r_i < r_a < r_0$ with $r_i = 0.1$ and $r_0 = 0.9$. The q profile is parabolic, satisfying the local value at r_0: $q = 0.854 + 2.184 r_a^2$. Model density and temperature profiles (equal for electrons and ions) are prescribed in terms of their gradients

$$R \nabla n_{e,i}(r) = n_e(r_0) \left. \frac{R}{L_n} \right|_{r_0} \mathcal{P}(r); \qquad R \nabla T_{e,i}(r) = T_e(r_0) \left. \frac{R}{L_T} \right|_{r_0} \mathcal{P}(r)$$

with the normalized profile, including boundary buffer zones, defined as

$$\mathcal{P}(r) = -1 + \text{sech}^2[(r - r_i)/(a\Delta r)] + \text{sech}^2[(r - r_0)/(a\Delta r)]$$

with width $\Delta r = 0.04$. For global codes the variable $\mathcal{P}(r)$ corresponds to the logarithm of the temperature or density. Any available energy, particle and momentum sources in the models are set to zero.

For global codes the proposed benchmark is a non-linear relaxation problem: given the ion temperature gradient as the only free-source, linear growth of ITG instabilities occurs, turbulence develops and saturates with the zonal flow dynamics, while the temperature profile consistently relaxes. A transport curve is the result, representing the ion thermal diffusivity as a function of the normalized ion temperature gradient. The Dimits fit for this curve (derived originally as a fit to the results of the LLNL gyrokinetic flux-tube PIC electrostatic turbulence code [1]), for this choice of L_n, is given by

$$\chi_i = 12.6 \left[1.0 - 6.0 \frac{L_T}{R} \right] \chi_{\text{GB}}, \tag{1}$$

in terms of the gyro-Bohm diffusivity $\chi_{\text{GB}} = \rho_s^2 c_s/a$, with $c_s^2 = T_e/M_D$ and $\rho_s^2 = T_e M_D/(eB)^2$ defined in terms of M_D, the actual deuterium mass.

Results presented here (section 4.1) scan the temperature gradient, with the other parameters fixed. The nominal value is scaled as $R/L_T \times \{1.0, 1.2, 1.5, 1.8\}$. Global code results are volume averaged over the outer third quarter radial domain. Local results are averaged over the entire domain.

2.2. Edge turbulence

A realistic representation of the edge turbulence regime requires the computations to follow $a \gg L_T \gg \rho_i$ and hence $R \gg L_T$. The latter inequality is extreme, it is enough to impose $R/L_T \sim L_T/\rho_i$ and $c_s/L_T > v_{\text{the}}/qR$ (with v_{the} the electron thermal velocity). This leads to the dimensionless definition of the edge regime, $\hat{\mu} \equiv (m_e/M_i)(qR/L_T)^2 > 1$, which implies strong non-adiabatic thermal electron activity. This edge zone is the last L_T inward of the last closed flux surface. Additionally, the drift Alfvén $\hat{\beta} \equiv (2\mu_0 p_e/B^2)(qR/L_T)^2 > 1$ (μ_0 being the magnetic constant) and collisionality $C \equiv 0.51(v_e L_T/c_s)\hat{\mu} > 1$ parameters define the inductive and resistive components of the parallel electron responses. With v_e, v_{the}/qR and c_s/L_T all comparable, the situation is referred to as transcollisional.

The standard case chosen for the edge turbulence code benchmark reflects these inequalities in a generic medium tokamak L-mode base case. Parameters are as follows: $n_e = 2 \times 10^{19}\,\text{m}^{-3}$, $T_e = 70\,\text{eV}$, $B = 2\,\text{T}$, $a = 0.5\,\text{m}$, $R = 1.65\,\text{m}$, $L_T = L_n = 0.0425\,\text{m}^{-1}$, $q = 3.5$, $\hat{s} = 1$, which correspond to $\hat{\beta} = 1$, $v_e L_T/c_s = 3$, $\hat{\mu} = 5$, $qR/L_T = 135$, $R/L_T = 40$ and $C = 7.65$. The values of $\hat{\beta} = \{1, 2, 3, 5\}$ and $C = 2.55 \times \{1, 2, 3, 5\}$ were varied. The global model benchmarked had to choose $q = 1.5 + 2r_a^2$ and set the n_e-profile such that $L_n = R/40$ in the center of the domain $r_0 - L_n/2 < r < r_0 + L_n/2$, with $r_0/a = 0.95$. Here, L_n was used as a proxy for L_T given that four-field models were used. Moreover, the global gyrofluid model used concentric circular model geometry as in the core cases given above. Profiles in edge turbulence codes must be maintained by sources as the confinement time of the layer is short [7]; the methods used to do this are documented in each of the codes' main references.

3. Description of the numerical models

A wide range of state-of-the-art numerical turbulence models ('codes') are active in the cross-verification, covering both gyrokinetic and gyrofluid codes using various numerical schemes. The benchmark is performed on non-overlapping codes, since often only one code per numerical approach or model was available. Gyrokinetic 'δf' codes separate the distribution function into fixed equilibrium and evolving perturbation pieces, whereas 'full-f' (also called 'total-f') codes effectively evolve both pieces self-consistently by not separating them. The underlying numerical approaches can be described as either Lagrangian, semi-Lagrangian or Eulerian. Particle-in-cell (PIC) models are Lagrangian, sampling the distribution function along phase-space trajectories with marker particles. The so-called 'continuum' or 'Vlasov' codes are Eulerian, evolving f on a fixed phase-space grid. The semi-Lagrangian scheme evolves the distribution function moving backwards in time along characteristics. Gyrofluid models evolve moments of the gyrokinetic equation, making use of appropriate closures. At the present time the gyrofluid models are based on an underlying δf gyrokinetic model, but retain the possibility to evolve the self-consistent profile as part of the dependent variable and thereby face the neoclassical equilibration of flows and currents. At the same level, all the δf-PIC codes also effectively evolve the profile as part of the 'perturbed f', while relying on the fact that for adiabatic core turbulence no density relaxation occurs.

The codes are merely listed according to type in the following; the reader is invited to refer to the referenced papers for detailed descriptions of the underlying models and implementations. In this study, all the (gyro-)fluid codes are 3D in space with various coordinate prescriptions. The gyrokinetic codes are all 5D, adding two velocity space dimensions in these cases corresponding to parallel velocity and magnetic moment.

Core turbulence models. GENE [4, 8] and GKW (Gyro-Kinetics@Warwick) [9, 10] are gyrokinetic δf Vlasov codes, involving an arbitrary number of particle species (both passing and trapped); GENE moreover includes pitch-angle and energy scattering collisions between any of them. The equations are electromagnetic and arbitrary flux surface shape is allowed (for GENE see [11]). For the present purpose they are run under a simplified local flux-tube model with a Maxwellian background.

The global gyrokinetic models tested are ORB5 [12, 13], a δf-PIC code with kinetic trapped electrons using 'thermostatting' dissipation [14], ELMFIRE [15], a full-f PIC code with both trapped and passing drift-kinetic electrons and collisions using a quasi-stochastic approach [16] and the GYrokinetic SEmi-LAgrangian full-f code GYSELA [17, 18]. Both GYSELA and ORB5 use canonical initial conditions for the equilibrium distribution function (see [19] for GYSELA). These codes all implement some variant of a general method to arrange the ion (particles) and electron (field) profiles to minimize large transients in the electrostatic $E \times B$ energy (this technique is becoming standard and is used even in gyrofluid models). Three (gyro-)fluid models have been tested. Various degrees of gyroaveraging are treated, but trapping along magnetic field lines is not included. The gyrofluid codes ETAI3D [20, 21] and GEM [22] correspond to δf global models keeping quadratic non-linearities. ETAI3D treats a three-variable adiabatic ITG model for core turbulence, while GEM started as a local edge model and now operates in core or edge, with a global-geometry version GEMR [23] suitable for either core or edge. CUTIE [24] implements a global two-fluid, electromagnetic Braginskii [25] model in the low-frequency limit. The background profile and fluctuations are separated into separate dependent variables, with the parameters however fully non-linear functions of the profile variables. The correspondence between gyrofluid equations with finite gyroradius non-linearities and low-frequency Braginskii equations is shown elsewhere [26].

In all the global models, profiles may be allowed to relax, or maintained by either sources or feedback control. In the present core tests they relax.

Edge turbulence models. For the edge turbulence case four fluid 'four-field' cold-ion electromagnetic models have been cross-verified. Although limited, this subset of Braginskii fluid equations [25] under the low-frequency approximation [27, 28] serves as a minimal standard for edge turbulence studies, following the dynamics of pressure, potential, current and parallel ion velocity, but not the temperatures. At this level, T_e is a background constant and $T_i = 0$, so that $p = p_e = T_e n_e$ hence pressure and electron density have identical roles, and the basic profile scale length $L_\perp$ is just L_n. Since there are not enough codes with more detail the comparisons were done at this level. The codes all use local or global versions of field-aligned coordinate geometry with a method to correct against the artificial ballooning effects caused by its naïve application [29], but with slightly different numerical implementations. DALF is a fluid model using an upwind numerical scheme [30]. TYR [31] is a fluid model which introduced the Arakawa [32]/Karniadakis [33] numerical scheme. This is especially suited to the Poisson-bracket structures represented by the non-linearities, treating vortex collision and merger processes especially accurately [34]. ATTEMPT [35] is a four-field model using this scheme, which also implements a model to treat ergodic flux surface perturbations induced by prescribed external currents [36]. GEM functions as a four-field model by restricting to the density and parallel gyrocenter moment variables of each species [37]. For this study the simplest version of toroidal geometry was used: a slab metric with magnetic shear, with toroidicity represented by the existence of magnetic curvature effects (diamagnetic and $E \times B$ compressibility). Due to the strength of the non-linear cascade dynamics, especially in density fluctuations towards small scale, all the codes apply

Table 1. Numerical parameters for the core test case $a/\rho_s = 184.7$ and $R/L_T = 8.28$: simulation domain size and spatial grid (for x, y, s see text), and velocity space grid (pertinent to gyrokinetic models, only).

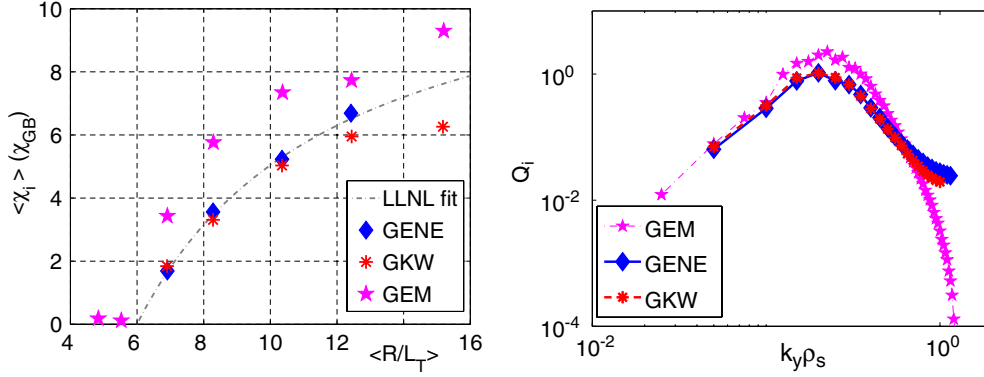|	L_x	L_y	L_s	N_x	N_y	N_s	$v_{\parallel \max}$	$\mu_{\max}$	$N_{v_\parallel}$	$N_{v_\perp}$
GENE	$127\rho_s$	$126\rho_s$	$2\pi q R$	128	48	16	$\pm 3 v_{th}$	$9\mu_{th}$	32	8
GKW	$128\rho_s$	$128\rho_s$	$2\pi q R$	83	21	16	$3 v_{th}$	$3 v_{th}$	32	8
GYSELA			$2\pi/4$	256	512	64	$\pm 6 v_{th}$	$7\mu_{th}$	64	8
	N_{part}									
ORB5	$320M$		2π	128	512	256	$\pm 5 v_{th}$	$\pm 5 v_{th}$		
ELMFIRE	$450M$		2π	91	150	8				
GEM	$100\rho_s$	$251\rho_s$	$2\pi q R$	64	128	16				
ETAI3D				512	256	128				
CUTIE				100	128	32				

Figure 1. (left) Transport curve for the core turbulence test case simulations: heat flux in gyro-Bohm units versus R/L_T. Flux-tube codes diffusivity values are averaged over a time period of about $1200 c_s/a$ after the overshoot phase of the simulation. The fit curve from [1] is reported as the dashed–dotted line. (right) Ion heat flux spectra as a function of $k_y \rho_s$ (on logarithmic scale), for the flux-tube codes in the standard case $R/L_T = 6.91$. Close agreement is found until the last few modes in the tail.

some form of high-wavenumber subgrid dissipation, implemented as described in the above references.

4. Simulation results and discussion

4.1. Core turbulence test case

The numerical parameters used by each of the codes for the core test case are reported in table 1: simulation box size, spatial grid, velocity space resolution, number of particles for the PIC codes. The coordinate description of the codes varies: field-aligned versions use the poloidal angle as the parallel coordinate s, with the drift angle y set such that k_y corresponds to nq/r where n is the toroidal mode number. Other versions use the poloidal and toroidal angles directly, referred to as y and s in the table, respectively. Different boundary conditions and dissipation buffers at radial boundaries are generally applied by the different codes.
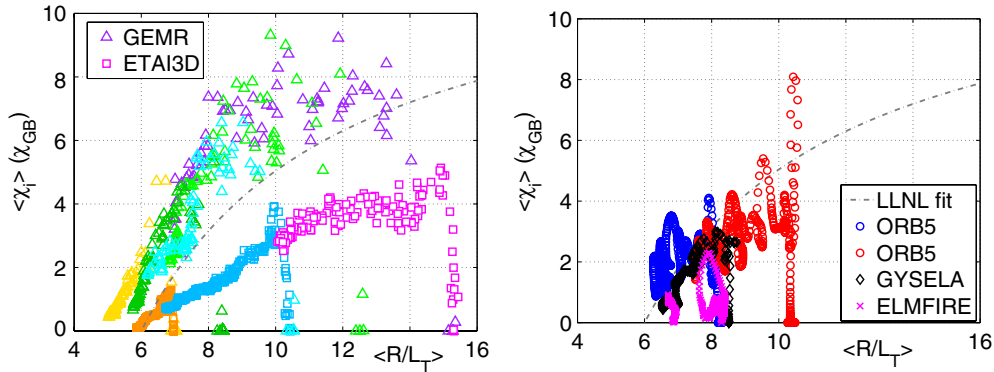
Figure 2. Ion heat flux in gyro-Bohm units versus R/L_T for the core adiabatic ITG test case for gyrofluid (left, triangles for GEMR code, squares ETAI3D) and gyrokinetic models (right, diamonds for GYSELA code, circles ORB5, crosses ELMFIRE). The time dependence has linear, overshoot, saturation and relaxation phases. The latter lies close to the fit curve from [1]. Slow transport-induced decay of the profile maps out the curve. Overlap of runs within the same model demonstrates the achievement of good time scale separation [22]. Volume averaging is as described in the text.

Flux-tube simulation results for adiabatic ITG turbulence obtained with the GEM, GENE and GKW codes are shown in figure 1. The ion heat diffusivity is averaged over a time interval of about 1200 c_s/a just after the overshoot phase. The two gyrokinetic codes, GENE and GKW, are in very good agreement and well reproduce the LLNL fit for US gyrokinetic flux-tube codes (1) [1]. The values obtained with the gyrofluid GEM code are somewhat higher, but still in reasonable agreement with the gyrokinetic ones. In particular, the non-linear upshift of the critical gradient is reproduced correctly. Global electrostatic simulations are shown in figure 2. The 'clouds' of points represent sampling of gradient and transport diffusivity values at successive time points following the decay of the profile. The time dependence has linear, overshoot, saturation and relaxation phases. The overlap of sets of points belonging to different runs (in figure 2 (left plot) in different colors) indicates that transport is temporally local and that although the length of simulations was shorter than a confinement time, good scale separation was achieved (cf [22]). Note that the gyrofluid simulation non-linear threshold agrees within the statistical scatter. GEMR overestimates the gyrokinetic flux-tube fit by 20% whereas the isotropic ETAI3D code runs predict lower values. It is to be noted that these two codes solve different model equations, ETAI3D using a simplified isotropic temperature equation, which possibly affects the zonal flow—GAM (geodesic acoustic mode [38]) saturation mechanism. The statistical variability of the heat conductivity values in the gyrofluid model corresponds well to the scale of bursts observed in the global gyrokinetic simulations.

ORB5 requested a very high number of particles for these decaying cases to be carried on for a sufficient duration for physical diagnosis before the noise level became dominant. With the thermostatting holding the profile stationary, however, the runs require fewer particles and may be carried on indefinitely and ORB5 finds diffusivity values in good agreement with the decay ones. This is circumstantial evidence for preferential dissipation of noise by the thermostatting. The results from GYSELA closely follow the LLNL fit. In GYSELA, *ad hoc* dissipative buffer regions allow for an efficient coupling of the plasma with the thermal bath at the radial boundaries. The resulting heat source does not always appear sufficient to counter balance the mean profile relaxation. Note that the averaging window was adjusted for both
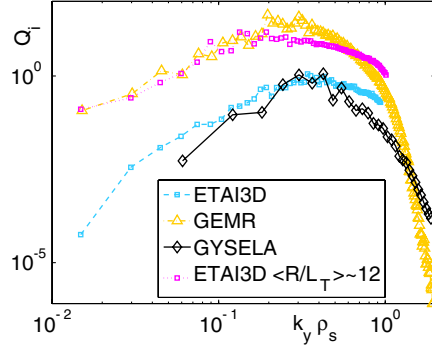
Figure 3. Ion heat flux spectra as a function of $k_y \rho_s$ (on logarithmic scale) for global core simulations with the gyrofluid codes ETAI3D (squares), GEMR (triangles) and gyrokinetic code GYSELA (black diamonds). The spectra are evaluated at the time for which $\langle R/L_T \rangle \simeq 6.9$ and $\langle R/L_T \rangle \simeq 12$ (the latter for ETAI3D code, dotted line).

ORB5 and GYSELA simulations in order to capture the region of maximal turbulent flux (data plotted in figure 2 (right plot) are averaged over $0.4 < r/a < 0.6$).

Results from ELMFIRE are somewhat lower than the fit in the overshoot phase, though the transient burst of turbulence relaxes quite rapidly. In the present test a sheared bipolar poloidal $E \times B$ flow is observed which suppresses turbulence and hence the associated transport. Its appearance has been traced back to flattening of radial pressure profile, related narrowing/widening of ion orbits and concomitant ion polarization in the cooling/heated regions. This neoclassical dynamics follows from the present lack of electron response due to electron adiabaticity over a relaxing full-f ion distribution with finite orbits. Additional dissipation might remove this dynamics, but would also result in unphysical damping of poloidal flows. However, it should be noted that GYSELA also contains these effects and the disagreement of those codes shows that this topic is still not settled.

Besides r.m.s. fluctuation time traces, toroidal (or k_y) spectra, poloidal (or parallel) envelopes for the vorticity, electrostatic potential and ion heat flux have been analyzed. From the envelopes one can observe that turbulence is more ballooned for higher gradients (i.e. far from threshold) and more slablike near the threshold. Spectra show evidence of the non-linear cascades to lower k_y in potential/density/flux and higher k_y in vorticity, for the stronger turbulence cases. Examples of ion heat flux k_y spectra are plotted in figure 1 (right plot) and figure 3, for local and global codes respectively. For the global code decaying cases the turbulence structure information is taken at the time point for which the evolving temperature gradient is close to the nominal value $\langle R/L_T \rangle = 6.9$. Note in figure 3 that since GYSELA simulations were performed on a quarter of torus only, the largest poloidal structures (low k_y) are underestimated. The non-linear cascade to lower k_y is evident in the higher temperature gradient case, as one can observe on the spectrum plotted for ETAI3D code at $\langle R/L_T \rangle = 12$.

The electromagnetic simulations were performed with the fluid codes GEMR and CUTIE, the latter setting all sources but the ohmic heating to zero. Since the prescribed safety factor profile has $q(0) < 1$, the generation of tearing modes is a critical issue for the electromagnetic models. GEMR simulations were performed ramping the gradient up to the prescribed value, avoiding strong Alfvén transients and switching off the tearing modes. A scan in β_e found transport levels close to the electrostatic cases until stabilization entered for $\beta_e > 10^{-3}$. The case $\beta_e = 4 \times 10^{-3}$ was completely stable. The case with the nominal $\beta_e = 5 \times 10^{-3}$ found higher kinetic ballooning modes which crashed the code
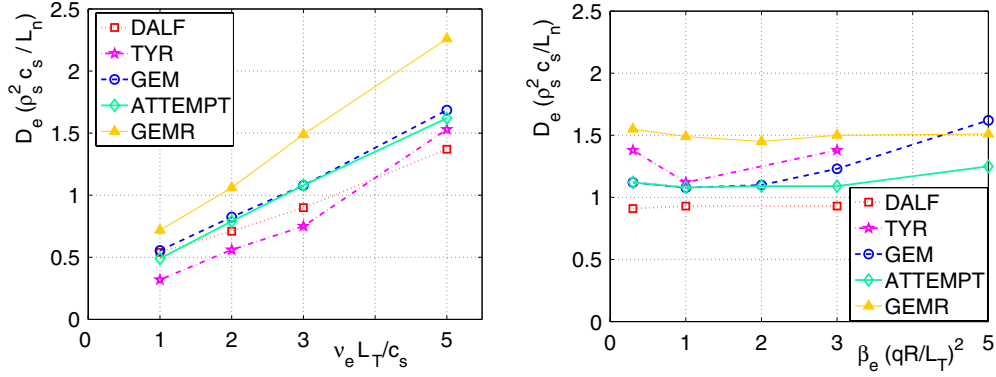
Figure 4. Transport dependence for the edge turbulence test case simulations: electron particle diffusivity D_e in units of $\rho_s^2 c_s/L_\perp$, versus collisionality $\hat{C} = \nu_e L_\perp/c_s$ (at fixed $\hat{\beta} = 1$) (left) and versus $\hat{\beta}$ (at fixed $C = 7.65$) (right). The D_e values are averaged over time from about $50a/c_s$ to the end of the run. For GEMR the value for $L_\perp$ is the volume averaged L_n.

before the turbulence could saturate. This general behavior is consistent with a previous flux-tube study using GEM [39]. Zonal potential profiles are found in close agreement with the neoclassical equilibrium [21, 40], with $n_e e \nabla_r \phi$ and $\nabla_r p_i$ partially cancelling and the difference made up by $B \nabla_\parallel (u_{i\parallel}/B)$. This is also found by both ETAI3D and GEMR in the electrostatic cases. CUTIE simulations used the prescribed profile, which has $q < 1$ near the axis. The $m = 1$ mode causes a very high burst of diffusivity, due to strong MHD activity, flattening the q-profile there and also causing a strong drop of the entire temperature gradient to values lower than the gyrokinetic non-linear threshold $R/L_T \sim 6$ (we note GEMR was found unable to function in the presence of this $m = 1$ instability). An effective conductivity equal to gyroBohm at the maximum gradient value $\langle R/L_T \rangle = 5$ after the sawtooth relaxation phase is predicted, whereas the effective threshold value is around $\langle R/L_T \rangle = 4.2$. GAM were not included in those runs, possibly affecting the saturation mechanism in the simulation as well as precluding the establishment of the neoclassical flow balances.

4.2. Edge turbulence test case

All the flux-tube codes used a grid of $64 \times 256 \times 16$ points over a domain of $20\pi\rho_s \times 80\pi\rho_s \times 2\pi qR$ in $\{x, y, s\}$, corresponding to the radial, the electron drift and the parallel directions, respectively. Timestep values were in the range of $0.01–0.05 L_\perp/c_s$. With the gradients being maintained, all the runs were found to saturate (all relevant time traces become stationary) within $500 L_\perp/c_s$, and data were taken beyond $1000 L_\perp/c_s$. The radial boundary conditions were Dirichlet in the dependent variables (cf [31]), corresponding to feedback control of the profiles. In GEMR the radial domain was as noted in section 2.2, and the entire flux surface was carried with 512 grid points in y (note L_y corresponds roughly to $2\pi r_0/q$). The gyrocenter density profiles were prevented from relaxing by dissipatively pinning their zonal averages densities to their prescribed initial profiles within an edge dissipation zone (cf [41]), another form of feedback control. Results for the collisionality and beta scans are shown in figure 4. They show agreement in trend and differences in detail. In the collisionality scan the flux-tube codes agree well whereas GEMR predicts higher particle diffusivity at higher C. It is to be noted that GEM and GEMR implement the same physics model but have flux-tube and global
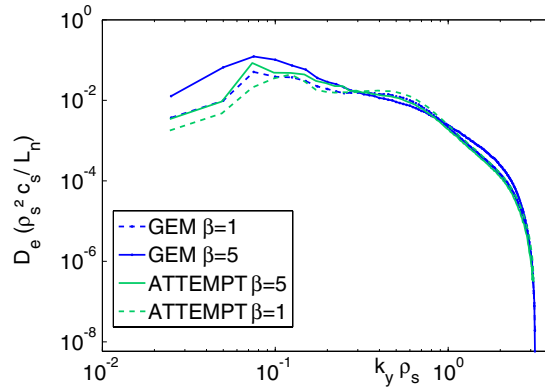
Figure 5. Electron particle diffusivity spectra as a function of $k_y \rho_s$ (on logarithmic scale) for the flux-tube codes ATTEMPT and GEM, for the edge test case $C = 7.65$, with $\hat{\beta} = 1$ (- - - -) and $\hat{\beta} = 5$ (——).

geometry (cf sections III and V of [29]), respectively. Larger scales play a larger role in the latter; diagnosis of this is ongoing. The beta scaling is essentially flat and the differences appear as details. Spectra of the electron particle flux versus k_y have also been computed and compared for all the flux-tube codes. An example of the remarkably good agreement between ATTEMPT and GEM codes is shown in figure 5.

5. Conclusion

Computation of turbulence and transport in magnetized plasmas is a difficult undertaking. A higher degree of confidence in predicting turbulent transport is gained by the mutual benchmarking of non-overlapping computational models, which, constrained by precisely the same test case prescriptions, produce results in good agreement. This is the case for the present cross-verification effort. Under the common test case of collisionless ITG driven turbulence with adiabatic electrons, core gyrokinetic and gyrofluid codes have shown a reasonable agreement of the predicted ion heat turbulent fluxes. The analysis of simulations in a statistical stationary state showing long-term saturation and the overlapping of decaying runs started at different temperature gradients ensures that heat flux bursts predictions are not artifacts. Diagnosing turbulence mode structure as well has allowed testing not only the integrated quantities but also the underlying physical processes. One has observed that the ITG instability evolves into turbulence, with the turbulent flux and the vorticity non-linearly cascading in different regions of the spectrum. This feature is well captured by the core gyrofluid simulations for high temperature gradients. Close agreement in the flux spectra has been found among the flux-tube models. There remain significant open issues involving the neoclassical flow equilibrium and its role in saturating the turbulence. Finally, in core turbulence runs with electromagnetic models the adiabatic response is essential in preventing an MHD character, leaving the fluxes themselves dominantly electrostatic despite the role of magnetic induction (finite β) in the parallel current responses. Comparisons between electromagnetic gyrokinetic models are left to the future.

The test of electromagnetic codes on L-mode edge plasma parameters is a new element of this cross-verification. Electron particle diffusivities predicted by the flux-tube edge codes have

been mutually validated by the collisionality and β scan, which show agreement in trends. For edge turbulence the non-adiabatic electron response is a central component and this has been well captured by the models used here. A remarkable agreement is found among the local ones both in fluctuation time traces and spectra. Moreover, the non-linear cascade process described above is clearly observed in the spectra for increasing collisionality and consistently reproduced by all the edge codes.

The present effort has not only allowed one to improve the numerical standards for turbulence simulations benchmarks but also opened the way to the investigation of a certain number of critical issues for global simulations, which will allow one to progress in the predictive capability of turbulent transport models. Among those is the self-consistency of equilibrium, which for the edge also includes magnetic fields and currents. Moreover, dissipation and saturation mechanisms involving zonal flows and geodesic curvature effects have a major impact on the turbulence level and therefore on any meaningful predictions.

Acknowledgments

References

[1] Dimits A M *et al* 2000 *Phys. Plasmas* **7** 969
[2] Nevins W M *et al* 2006 *Phys. Plasmas* **13** 122306
[3] Nevins W M *et al* 2007 *Phys. Plasmas* **14** 084501
[4] Jenko F *et al* 2000 *Phys. Plasmas* **7** 1904
[5] Becoulet A *et al* 2007 *Comput. Phys. Commun.* **177** 55–9
[6] Terry P *et al* 2008 *Phys. Plasmas* **15** 062503
[7] Scott B 2005 *Phys. Plasmas* **12** 082305
[8] Dannert T and Jenko F 2005 *Phys. Plasmas* **12** 072309
[9] Peeters A and Strinzi D 2004 *Phys. Plasmas* **11** 3748
[10] Peeters A G *et al* 2007 *Phys. Rev. Lett.* **98** 265003
[11] Xanthopoulos P and Jenko F 2006 *Phys. Plasmas* **13** 092301
[12] Jolliet S *et al* 2007 *Comput. Phys. Commun.* **177** 409–25
[13] McMillan B F *et al* 2008 *Phys. Plasmas* **15** 052308
[14] Krommes J A 1999 Thermostatted delta-f *Phys. Plasmas* **6** 1477
[15] Heikkinen J A *et al* 2008 *J. Comput. Phys.* **227** 5582–609
[16] Sosenko P P *et al* 2001 *Phys. Scr.* **64** 264
[17] Grandgirard V *et al* 2007 *Plasma Phys. Control. Fusion* **49** B173–82
[18] Grandgirard V *et al* 2008 *Commun. Nonlinear Sci. Numer. Simul.* **13** 81–7
[19] Dif-Pradalier G *et al* 2008 *Phys. Plasmas* **15** 042315
[20] Ottaviani M and Manfredi G 1999 *Phys. Plasmas* **6** 2367
[21] Falchetto G L *et al* 2007 *Phys. Plasmas* **14** 082304
[22] Scott B D 2005 *Phys. Plasmas* **12** 102307
[23] Scott B D 2006 *Contrib. Plasma Phys.* **46** 714

[24] Thyagaraja A 2000 *Plasma Phys. Control. Fusion* **42** B255
[25] Braginskii S I 1965 *Rev. Plasma Phys.* **1** 205
[26] Scott B D 2007 *Phys. Plasmas* **14** 102318
[27] Hinton F L and Horton C W 1971 *Phys. Fluids* **14** 116
[28] Wakatani M and Hasegawa A 1984 *Phys. Fluids* **27** 611
[29] Scott B D 2001 *Phys. Plasmas* **8** 447
[30] Scott B D 2000 *Phys. Plasmas* **7** 1845
[31] Naulin V 2003 *Phys. Plasmas* **10** 4016
[32] Arakawa A 1966 *J. Comput. Phys.* **1** 119
     Arakawa A 1997 *J. Comput. Phys.* **135** 103–14 (reprint)
[33] Karniadakis G E *et al* 1991 *J. Comput. Phys.* **97** 414
[34] Naulin V and Nielsen A H 2003 *SIAM J. Sci. Comput.* **25** 104–26
[35] Reiser D 2007 *Phys. Plasmas* **14** 082314
[36] Reiser D and Scott B D 2005 *Phys. Plasmas* **12** 122308
[37] Scott B D 2003 *Plasma Phys. Control. Fusion* **45** A385
[38] Winsor N *et al* 1968 *Phys. Fluids* **11** 2448
[39] Scott B D 2006 *Plasma Phys. Control. Fusion* **48** B277
[40] Ribeiro T T and Scott B 2008 *Plasma Phys. Control. Fusion* **50** 055007
[41] Ribeiro T T and Scott B 2005 *Plasma Phys. Control. Fusion* **47** 1657